Journal of Instrumentation

PAPER • OPEN ACCESS

Module development for the ATLAS ITk pixel detector

To cite this article: S. Möbius and on behalf of the ATLAS ITk Group 2022 *JINST* **17** C03042

Published by IOP Publishing for Sissa Medialab

Received: *September 30, 2021*
Accepted: *December 6, 2021*
Published: *March 28, 2022*

22$^{\text{ND}}$ International Workshop on Radiation Imaging Detectors
June 27–July 1, 2021
Ghent, Belgium

Module development for the ATLAS ITk pixel detector

S. Möbius on behalf of the ATLAS ITk Group

II. Physikalisches Institut, Georg-August-Universität Göttingen,
Friedrich-Hund-Platz 1, 37075 Göttingen, Germany

E-mail: silke.moebius@phys.uni-goettingen.de

Abstract: After the upgrade of the LHC to the high-luminosity-LHC, the instantaneous luminosity will reach unprecedented values, resulting in about 200 proton-proton interactions in a typical bunch crossing. The current ATLAS inner detector will be replaced by an all-silicon system, the Inner Tracker. The innermost part of the Inner Tracker will consist of a state-of-the-art pixel detector. The individual modules of the Inner Tracker pixel detector comprise silicon sensors using various different technologies, with the sensors readout using the new ITkPix ASIC.

Keywords: Hybrid detectors; Particle tracking detectors (Solid-state detectors); Radiation-hard detectors

2022 JINST 17 C03042

https://doi.org/10.1088/1748-0221/17/03/C03042

Contents

1 Introduction

The integrated luminosity of the LHC [1] is planned to be increased by a factor of ten compared to the design luminosity of the LHC by 2027. The so-called High Luminosity-LHC (HL-LHC) will result in an increased particle density in the experiments, which results in a higher occupancy in the detectors and a higher radiation damage. In order to tackle this problem, the current detectors of the experiments need to be replaced by radiation harder, faster detectors of higher granularity.

For this paper of interest is the inner detector of the ATLAS experiment [2] which is upgraded to an all-silicon system, the Inner Tracker (ITk) [3, 4], as seen in figure 1(a). There will be a four-layered new strip detector with planar sensors and a five-layered hybrid pixel detector covering an area of 13 m^2, which features $\approx$10000 hybrid modules, on inner layers with 3D sensors and outer layers with planar sensors. The focus here lies on the hybrid pixel detector.

To produce hybrid pixel detector modules, silicon sensors are bump bonded to a readout chip (front-end chip), forming a bare module as can be seen in the microscope image in figure 1(b). The signal from traversing particles is produced in the sensor volume and transmitted via the bump-bond to the readout electronics. Currently, the RD53A prototype readout chip [5] that was jointly developed with CMS is used for extended studies while the first versions of the final readout chip ITkPixV1 are being validated to pave the way for the final version ITkPixV2 [6].

A full pixel detector module consists of a bare module glued and wire-bonded to a flexible printed circuit board (flex).

2022 JINST 17 C03042

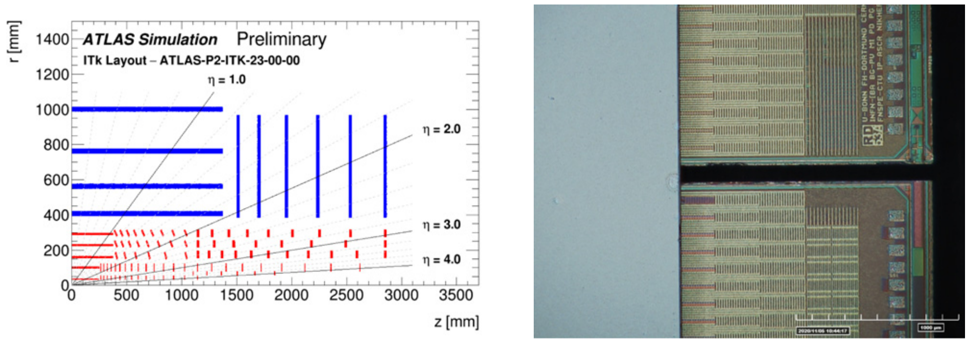

a) b)

Figure 1. The ITk pixel detector will have five layers of hybrid pixel sensors where readout chips are bump-bonded to sensors. (a) The layout of the ITk, showing the pixel detector in red and the strip detector in blue (taken from [4]). (b) RD53A bare module showing the edges of two chips and the sensor.

2 Module types and bare components

Depending on the module type, there are 3 or 4 readout chips powered in parallel. Planar quad modules have four readout chips and a silicon pixel sensor with a pixel pitch of (50×50) µm^2. The active thickness is 100 µm for the innermost layer and 150 µm for all layers further outside. The size of the sensor is $\approx(4 \times 4)$ cm^2 and the sensors are n-in-p sensors to slow down degradation under irradiation. Compared to pixel modules on the current pixel detector with n$^+$-in-n sensors type inversion at high irradiation doses cannot occur, thus making it possible to operate the detector for many years under difficult conditions as present in the inner layers of the ITk. Triplet modules have three readout chips and are built with 3D sensors of 100 µm active thickness and an area fitting the size of the readout chips. These have a pitch of (50×50) µm^2 and an area of $\approx (2 \times 2)$ cm^2.

The layouts of the modules and the positions of the sensors and readout chips are shown in figure 2.

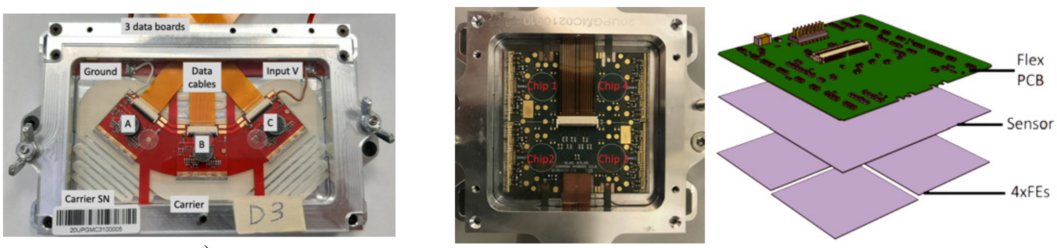

a) b)

Figure 2. A triplet module and a quad module, showing the different positions of the sensors and especially the readout chips. (a) An assembled triplet module. (b) An assembled quad module and the exploded view of the schematics of a quad module.

2022 JINST 17 C03042

In order to build functioning modules, the components need to be tested thoroughly. This means that sensor, readout chips and flex of each module must be declared as working before actually proceeding to the module building step.

For the sensors, a market survey was conducted to help finding vendors for ITk pixel sensor production. Chosen foundries were asked to produce Single Chip (SC) and Double Chip (DC) sensors which satisfy the ITk specifications. The areas are $\approx(1 \times 2)\,\mathrm{cm}^2$ for SC and $\approx(1 \times 4)\,\mathrm{cm}^2$ for DC prototypes. Their performance was evaluated in tests in laboratories, which comprise visual inspection, electrical and mechanical tests and test beam measurements of SC sensors at DESY.

Visual inspection is performed by eye, with a microscope and a camera, depending on the equipment in the institutes. It is necessary to check for debris on the surface or defects on the surface or the chip edges to understand the origin of possible failures in the tests to be performed afterwards.

Electrical tests in the laboratories include current-voltage (*IV*) characterisation (at 20 °C and relative humidity (RH) <50%), current-time (*It*) measurements for 48 h and capacitance-voltage (*CV*) characterisation. These tests are performed with probe needles and environmental control. One possible set-up is a semi-automatic probe station with temperature controlled chuck, as can be seen in figure 3(a). Example results for three quad bare modules are shown in figure 3(b).

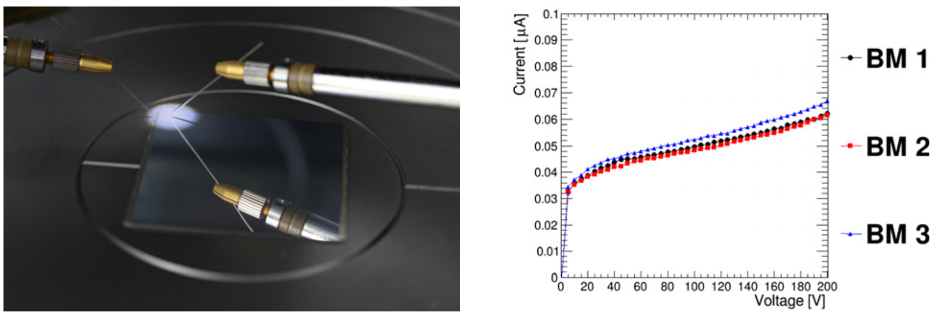

a) **b)**

Figure 3. *IV* measurements and results of bare RD53A modules on a semi-automatic probe station. (a) Probing of an RD53A bare module. (b) Bare module *IV* results for three bare modules.

The laboratory tests are repeated after irradiation to mimic the conditions at the end-of-lifetime. Sensor measurements are performed at −25°C as they will also be in a cold environment in the detector to reduce the leakage current in the depleted silicon bulk that is generated by thermal excitation and scales with temperature. The leakage currents need to be as low as possible to allow to measure the currents generated by a passing particle. Another effect that can be observed is the change of leakage current with annealing time and temperature, which describes the time the sensors have been in a warm environment. During annealing, defects in the sensor can repair partially and thus the leakage current caused by irradiation can decrease. Due to this, the sensors need to be stored in cold conditions after irradiation to allow an assessment of the performance right after irradiation.

Mechanical measurements are needed to assure that the sensors can be bump-bonded to the readout chips and thus evaluate the thickness and the bow of the sensors by using automated or

2022 JINST 17 C03042

non-automated microscope measurements which measure the height with laser measurements or by adjustment of the focus of an optical microscope. The limits are given for the bow to be <12.5 µm and for the thickness variation to be <15 µm.

Additionally to the laboratory tests on the bare sensors, test beam measurements were performed at DESY with a 5 GeV electron beam. In order to test a sensor, it is first bump-bonded to form a sensor — readout-chip hybrid, which is then wire-bonded to a rigid printed circuit board to assemble a SC module. In figure 4, measurements from a 150 µm thick sensor with a pixel pitch of (50×50) µm^2 are shown for a 4×4 pixel region. It received irradiation fluences of $\Phi = 5 \times 10^{15}$ $n_{eq}cm^{-2}$ and was measured at $V_{bias} = 600$ V with a low leakage current of $I_{leak} = 20.2$ µA.

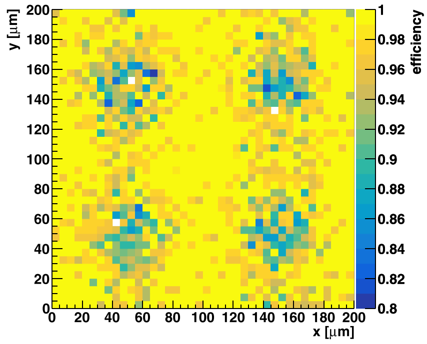

Figure 4. Test beam results for a thick sensor irradiated to a fluence of $\Phi = 5 \times 10^{15}$ n_{eq} cm^{-2} showing a very good performance.

The measurement of interest is the hit efficiency at perpendicular incidence measured in a beam telescope. It is defined as:

$$\text{Efficiency} = \text{tracks in region with matched hit in DUT/total tracks in region.}$$

A pattern is visible which originates from the bias grid, which was implemented on the sensor surface, connecting every pixel and thus allowing to test the full sensor when it is not yet bump-bonded to a readout chip. The fiducial efficiency is the efficiency in the fiducial region, which is dependent on the sensor design and in the case with bias grid the region where there is no disturbance of the sensor measurements due to bias dots.

With the requirement of the market survey for the highly irradiated sensors to have an efficiency $>97\%$ when biased with 600 V, this sensor with an efficiency of $(97.78 \pm 0.06)\%$ and a fiducial efficiency of $(99.68 \pm 0.06)\%$ meets the requirements.

3 Quad module assembly of bare module and flex

As mentioned above, modules, comprising a flex and bare modules, are built for the different layers of the detector. The tooling for the assembly process, i.e. the flex-to-bare-module attachment for quad modules has been developed in Göttingen for the whole ITk pixel collaboration.

2022 JINST 17 C03042

It consists of two jigs that carry the flex and the bare module using vacuum suction. With dowel pin alignment the correct positioning of the components to each other is assured, allowing to place them on top of each other with ±50 µm precision.

3.1 Module building specifications

With an additional stencil tool, which comprises a stencil frame and stencil sheet, a predefined amount of glue can be spread on the flex before closing the tooling for attachment and curing. With adjustment screws on the tooling the distance between the jigs is adjusted, allowing to control the height of the glue, which is specified to be (40 ± 15) µm. The calibration is done with a bare module + flex + 40 µm precision steel foil as glue spacer. This value is defined such that the module envelope fits in the limited space in the pixel detector layers. Apart from the space the adhesive must also be properly spread between the components to ensure that the module components do not de-laminate. The tooling and an example of spreading the glue can be seen in figure 5.

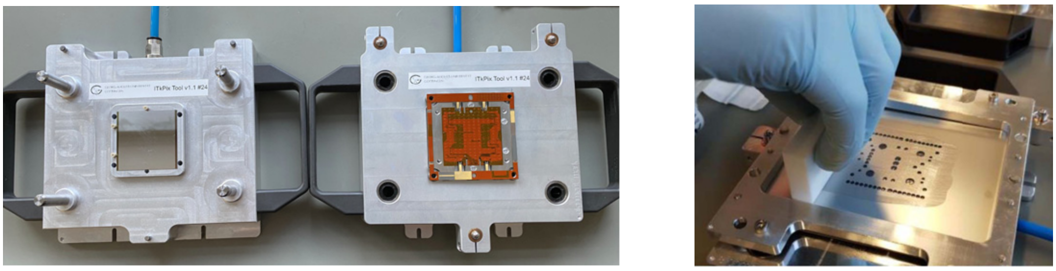

a) **b)**

Figure 5. The module assembly is performed with a common tool, allowing precise mating of two jigs and thus assembly of a module with 50 µm precision. (a) Quad module tooling consisting of two jigs, one holding the bare module and the other the flex (with glue applied in this case). (b) Application of the glue with the spatula on the stencil sheet.

Where initial gluing patterns were optimized to provide as little glue as possible onto the flex to just allow proper wire bonding and further handling of the module, this was observed to lead to de-lamination after thermal cycling which is something that can happen during normal detector operation due to cooling failures as well as planned cool and warm times of the detector modules. An improved glue pattern which aims at providing full glue coverage is defined to match the glue thickness. Higher glue thicknesses lead to a much reduced glue coverages which can result in de-lamination more likely.

In order to assure proper wire bonding, not only the wire bonding pads need to be properly glued to the sensor, but also the x-y-alignment needs to be within specifications. As for the mechanical measurements on the sensors, a microscope was used for all the measurements. A module needs to be attached with a precision of ±50 µm in x and y with the specifications of the flex and Si-dummy shown in table 1.

2022 JINST 17 C03042

Table 1. Specifications of the flex and the Si-dummy.

	y-dim.	x-dim.	Height	Planarity
Si-dummy	41.1 mm	42.2 mm	325(+55 -40) µm	±25 µm
Flex	40.6 mm	40.4 mm	160 ± 20 µm	

With the setting of the glue height not being ideal, a new tooling for ITkPix chip modules is ongoing, providing an easier and more precise mechanism to mate the jigs and thus the module components.

3.2 Parylene coating, wire bonding and pull testing

Before sending the modules to testing, Parylene is applied to protect the module and especially the wire bonds. Masking tape and cover are attached to the backside of the module and the extended connector area, see figure 6. This is done before Parylene coating of wire bonds to make sure that the Parylene only reaches the wire bonds which it is supposed to cover to prevent destruction and assure HV-protection.

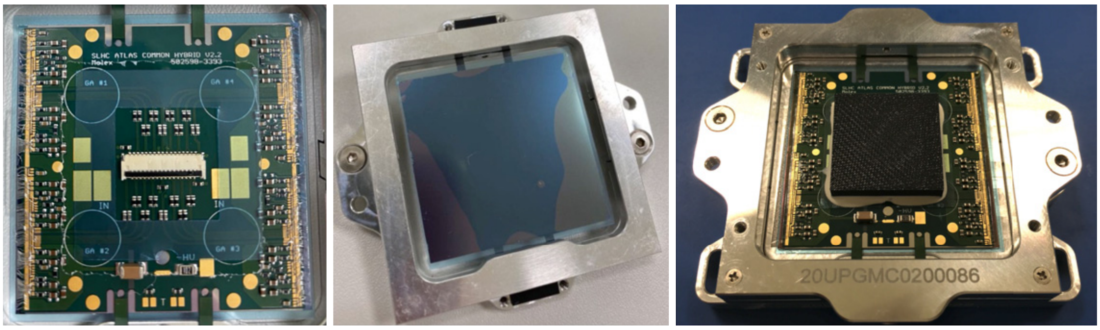

Figure 6. Tape and cover are added before Parylene coating to make sure only wire bonds are covered with Parylene to prevent destruction and assure HV-protection.

A crucial part of the module building is the wire bonding, connecting the readout chips to the flex, providing the electrical connection to allow the readout of the modules. Two methods to verify bond quality are performed for every single module. In a visual inspection with a microscope the status of the bonds is checked by looking for mis-bonded wires and assessing the shape of the wire bonds. All wires should be in a straight line between the bond pads and have wire loops which are uniform and without kinks. Apart from that, no wires must be touching each other. Destructive tests performed on wires which are not necessary for the module operation are pull tests where the quality of bonds is checked by measuring the force it takes to rip off a wire. To evaluate the overall behaviour of a modules, 32 pull tests are carried out on each module (8 per chip). Figure 7 shows the pull head used for the pull tests and gives an impression of properly bonded wire bonds.

2022 JINST 17 C03042

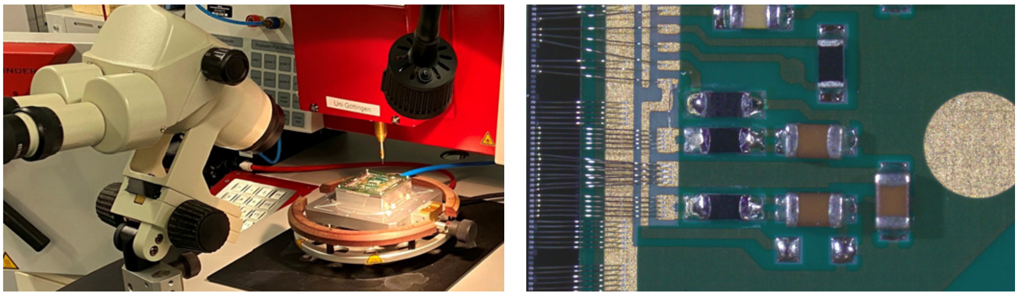

Figure 7. Inspection of wire bonds and pull tests with the pull head on a wire bonding machine.

4 Module testing

The development of the testing infrastructure has been performed with the preliminary RD53A readout chip, which is diced to match the size of the final ItkPixV2. In a staged approach for the electrical qualification of modules, the participating institutes have built up their infrastructure and proven to be capable of testing modules. The quad modules stay in a common module carrier for protection of wire bonds during shipping and testing.

A general testing procedure comprises tuning of the readout chips of each module and especially of every separate Front-End (FE) and scans of the FEs. With three different FE designs in the RD53A readout chip this asks for a specified tuning procedure, adapted to each FE design. In figure 8, tuning examples for one readout chip are given, showing the threshold and the Time-over-Threshold (ToT) distribution. With a set threshold of 1000 electrons (e) and a ToT of 7 bunch crossings (bc), the results confirm that the response of the readout chip is according to expectations.

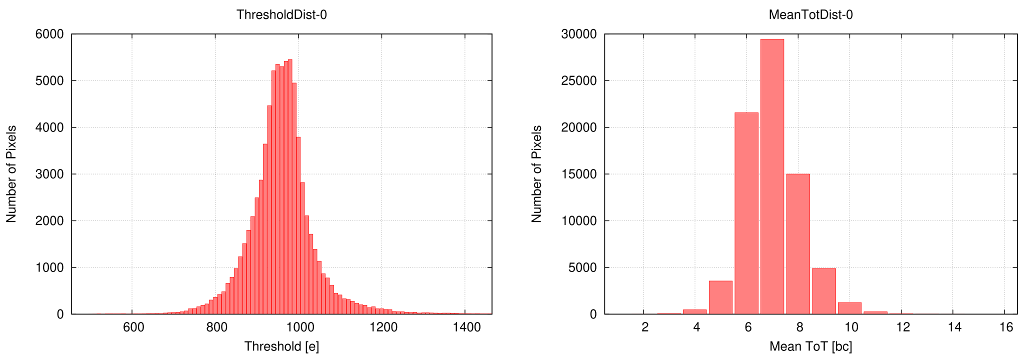

Figure 8. Chips on an RD53A quad module tuned to a threshold of 1000 electrons and a ToT of 7 bunch crossings.

In order to maintain the safety of the modules, the monitoring of environmental parameters, voltages and currents is crucial and has to trigger an interlock when crossing the set thresholds for safe module operation. In order to set the conditions of the tests on the quad modules, a common cooling unit designed in the University of Bergen is used in most of the participating institutes.

2022 JINST 17 C03042

Using a vacuum chuck with cooling by an external chiller and a Peltier element housed inside a foam box the modules can be brought to the desired temperatures at which the testing is supposed to be performed. To understand the performance of the modules in detail, tests are performed at 30 °C, 20 °C and −15 °C. Power cables, data cables, vacuum and dry air supply tubes are routed through the foam housing.

Thermal cycling is a very important test to mimic and understand the behaviour expected from a possible failure of CO_2 cooling in the actual ITk detector in the ATLAS detector. Different types of cycles are used: one cycle down to −55° and 10 cycles down to −45°C. For these tests it is very important to keep dry conditions in the cooling unit to avoid condensation.

Source scans with a radioactive source are also performed to validate the functionality of the sensor pixels. Only when the bump bonding connection between the sensor and the readout chip is functioning signals from the sensor can be transmitted. Especially at the early stages of module building where the hybridization procedure needs to be qualified and understood, these scans are a valuable tool.

While most of the tests could only be performed with RD53A modules, the recent arrival of modules with a newer chip version, ITkPixV1.1, allowed checks of these chips to see if the changes in the design as compared to the RD53A preliminary chips led to improvements. As no bump-bonded sensor to readout chip bare modules were available at the time of the conference, only results from tests on digital modules can be shown. Digital modules have readout chips but not real sensor. In the plots of figure 9 good threshold and noise behaviour can be seen, as expected.

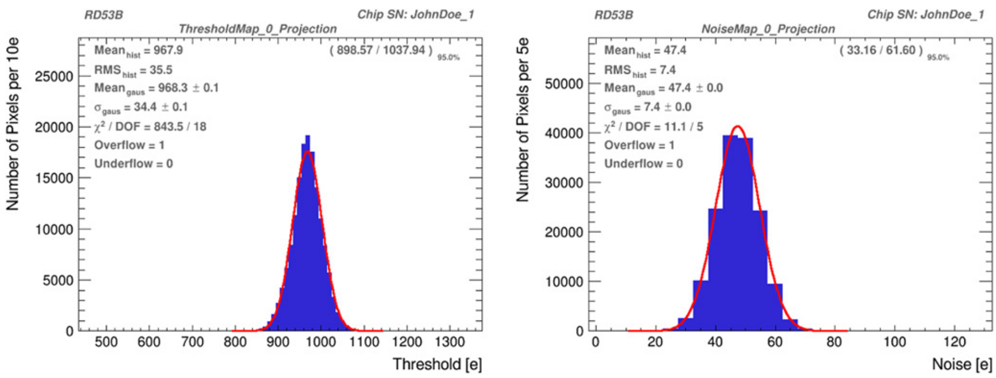

Figure 9. First results of digital modules with ITkPixV1.1 readout chips showing very clean threshold and low noise behaviour.

5 Conclusion

With the sensor market survey being finalized and the tendering for production ongoing, the ITk module building efforts are advancing towards pre-production for the ITk. Currently, the module building and testing efforts with the preliminary quad modules using an RD53A readout chip are running, in order to provide a sufficient amount of working modules for further system tests while in parallel the final version of the readout chip is tested to understand the behaviour in more detail.

2022 JINST 17 C03042

Acknowledgments

Test beam results are a common effort from the ITk Planar Pixel Market Survey Test Beam Reconstruction Team. The measurements leading to these results have been performed at the Test Beam Facility at DESY Hamburg (Germany), a member of the Helmholtz Association (HGF).

References

[1] L. Evans and P. Bryant, *LHC machine,* 2008 *JINST* **3** S08001.

[2] ATLAS collaboration, *The ATLAS experiment at the CERN Large Hadron Collider,* 2008 *JINST* **3** S08003.

[3] ATLAS collaboration, *Technical design report for the ATLAS Inner Tracker pixel detector*, Tech. Rep., CERN-LHCC-2017-021, ATLAS-TDR-030 CERN, Geneva (2017), https://cds.cern.ch/record/2285585.

[4] ATLAS collaboration, *Technical design report for the ATLAS Inner Tracker strip detector*, Tech. Rep., CERN-LHCC-2017-005, ATLAS-TDR-025 CERN, Geneva (2017), https://cds.cern.ch/record/2257755.

[5] RD53 collaboration, *The RD53A integrated circuit*, Tech. Rep., CERN, Geneva (2017), https://cds.cern.ch/record/2287593.

[6] RD53 collaboration, *RD53B manual*, Tech. Rep., CERN, Geneva (2019), https://cds.cern.ch/record/2665301.